Dielectric investigation of electrically oriented ferroelectric smectic mixture CS-1013

S. K. Kundu,[1] E. Okabe,[2] W. Haase,[3] and B. K. Chaudhuri[1,*]
[1]*Solid State Physics Department, Indian Association for the Cultivation of Science, Kolkata-700032, India*
[2]*Specialty Chemicals Research Center, Chisso Petrochemical Corporation, 5-1 Goikaigan Ichihara Chiba, 290-8551, Japan*
[3]*Department of Physical Chemistry, Technical University Darmstadt, Petersen Strasse 20, Darmstadt, Germany*
(Received 21 February 2001; published 24 October 2001)

From dielectric spectroscopic study, a first-order ferroelectric phase transition has been observed in ferroelectric smectic mixture CS-1013 having the phase sequence Cr-Sm*C**-Sm*A*-*N**-Iso. Frequency (100 Hz–10 MHz) and temperature-dependent dielectric measurements have been performed on an electrically aligned sample (thickness 15 ± 1 μm) gold coated on glass plates. In the unidirectionally aligned sample, two dielectric relaxation modes (Goldstone mode and soft mode) have been clearly observed in the ferroelectric Sm*C** phase while only one relaxation mode (soft mode) is visualized in the paraelectric Sm*A* phase. Low-frequency molecular relaxation was also observed in the smectic phases. The experimental results have also been analyzed at different temperatures and biasing voltages for an understanding of the dynamics of dielectric processes in the ferroelectric phase. Finally, we proposed the ''pseudospin'' model for understanding the ferroelectric-antiferroelectric transition in liquid crystals. We associate the tilt angle θ and the pitch of the helix, respectively, with biaxial (b) and uniaxial (u) anisotropy parameters as fluctuating parameters around their stability limit (corresponding to the crystalline values). Here, the director acts as the pseudospin variable. This gives rise to a transverse Ising type (or anisotropic Heisenberg model under the mean-field approximation). It is then shown that such a model with fluctuations of (b) and (u) would explain the ferroelectric and antiferroelectric phase transitions in such liquid crystals. Using Landau theory and the stability conditions, we have also shown, in brief, the feasibility of different types of phase transitions in the ferroelectric liquid crystal system.

DOI: 10.1103/PhysRevE.64.051708 PACS number(s): 77.22.Gm, 77.84.Nh, 64.70.Md

I. INTRODUCTION

After the discovery of ferroelectricity in some liquid crystals [1,2], it has become one of the most attractive fields of current research on ferroelectric liquid crystals (FLC) because of their technological, as well as fundamental interests. Study of dielectric response in FLC showing the Sm*C**-Sm*A* phase transition [3–9] indicated two main relaxation modes. One is the Goldstone mode (GM) in the Sm*C** phase arising because of the phase fluctuations in the azimuthal orientation of the director in the vicinity of Sm*A*-Sm*C** transition point. The other mode is the soft mode (SM), which appears only at a transition temperature and a few degrees below the transition temperature in the Sm*A* phase. The soft mode appears because of the fluctuation of the amplitude of the tilt angle. It has also been shown theoretically and experimentally [10] that in a FLC mixture, the SM may appear in both phases very close to the transition temperature (Sm*C**-Sm*A**). While studying the phase transitions in FLC, it has also been observed that mainly two types of ferroelectric liquid crystals are generally found. The first one showing second-order phase transition has the phase sequence from crystalline (Cr) to a highly ordered smectic phase such as SmH, Sm*I*–chiral smectic *C* (Sm*C**)–smectic *A* (Sm*A*)–chiral nematic (*N**)–isotropic (Iso). On the other hand, the second type of FLC showed first-order phase transition has the phase sequence of Cr-Sm*C**-*N**-Iso. The FLC showing first-order phase transitions are very interesting and important as these materials have a large tilt angle (θ) that do not depend greatly on the temperature and, therefore, these FLC materials could be good candidates for preparing Electro-optical switches [11], guest-host displays [12], etc. It has already been shown that in a FLC, the Landau model for the free energy may be expressed as $F=\eta P_s^2-\varphi P_s\theta-\gamma\Omega P_s^2\theta^2+\delta P_S^4$ where η, γ, and δ are constants, φ is the piezoelectric bilinear coupling coefficient [13], and Ω is the biquadratic coupling coefficient inducing a transverse quadrupole coupling.

In the present paper, we report the dielectric spectroscopic study in a typical FLC (viz. CS-1013) in the Sm*C**-Sm*A* phase—showing first-order phase transition and having the following phase sequence, viz.,

Cr-*U*.*K*-Sm*C**-63 °C-Sm*A*-70 °C-*N**-80 °C-Iso.

Frequency (100 Hz–10 MHz) and temperature (29–82 °C) dependences of different modes have been investigated. The FLC of our present paper is particularly important because the ferroelectric transition (crystalline to chiral phase) temperature (~35 °C) of the sample is very close to room temperature. We have also suggested a pseudospin-type model for the phenomenological explanation of the ferroelectric phase transition in FLC by considering fluctuations of the model parameters associated with the tilt angle.

II. EXPERIMENT

The ferroelectric smectic mixture CS-1013 used for the present measurement was prepared by Chisso Petrochemical Corporation, Japan. The basic parameters of this FLC are shown in Table I. The shielded parallel-plate capacitor hav-

*Author to whom correspondence should be addressed

TABLE I. Some important parameters of the CS-1013 ferroelectric liquid crystal.

Spontaneous polarization (P_s)	25 °C	-15.0 nC cm^{-2}
Tilt angle (θ)	25 °C	26°
Helical pitch in the N^* phase	$\sim T_N$[a]	38 μm
Helical pitch in the SmC^* phase	25 °C	6 μm
Response time (τ)	25 °C, $E=\pm 10$ V/μm	739 μsec
Rotational viscosity (η[b])	25 °C	1282 mPa s
Optical anisotropy (Δn)	25 °C, $\lambda=546$ nm	0.12

[a] T_N means N^*-SmA just above transition temperature.
[b] $\eta_0=\eta/\sin^2\theta$.

ing a thickness of (15 ± 1) μm was used for dielectric measurements. Gold-plated electrodes were made on glass plates by the sputtering technique. The active area of the cell is 35 mm^2. The cell was filled with the desired FLC sample by the capillary action technique in an isotropic phase [14]. We used a stabilized low-frequency ac ($\sim$1.67 kV/cm) field for better alignment of the sample for about 75 minutes. Dielectric measurements were carried out by a computer-controlled Hewlett Packard 4192A impedance analyzer having a frequency range of 5 Hz–13 MHz. The temperature of the sample (between 25 and 85 °C) was controlled by a Eurotherm (Germany) controller with an accuracy of ±0.1 °C.

III. RESULTS AND DISCUSSION

A. Dielectric study

In the following paragraphs, we discuss the dielectric relaxation processes in the SmA-SmC^* phase of the ferroelectric smectic mixture (CS-1013) which exhibited spontaneous polarization at the temperature 25 °C ($P_s=-15.0$ nC cm^{-2}). To study the dielectric relaxation processes showing up in the SmC^* phase due to the Goldstone mode, precise measurements of the complex dielectric permittivity ($\varepsilon^*=\varepsilon'-i\varepsilon''$) have been made in the frequency range 100 Hz to 10 MHz. Figure 1 represents the temperature dependence of the imaginary part of dielectric permittivity (ε'') obtained at two different frequencies (1 and 10 kHz) for the Iso, N^*,SmA,SmC^*, and crystalline phases. It is seen from this figure that the SmA-SmC^* phase transition is very strong (large shift). Figure 2 showed the real part of dielectric permittivity (ε') in the SmC^* phase, without bias field, as a function of frequency for three different fixed temperatures. The contribution of ε' is coming from the Goldstone mode for the ferroelectric smectic mixture (CS-1013). It is observed that the Goldstone mode is present upto the SmA-SmC^* phase-transition point. It is interesting to note that after applying a bias field of 1 V/15 μm, there is a certain change in the dispersion curve. Figure 3, obtained for the SmC^* phase, indicated strong bias field dependence of the dispersion curve. In Fig. 4, we have shown a typical plot of the imaginary part of dielectric permittivity (ε'') as a function of frequency at three different temperatures for the SmC^* phase. This figure also exhibits the presence of three relaxation modes, namely, Goldstone mode, soft mode, and molecular mode. Interestingly, for the SmA phase (Fig. 5), we see that the Goldstone mode has disappeared. This is because of the low-frequency relaxation caused by the ion present in this sample. The experimental ε'' data are fitted with the following equation [15,16]:

$$\varepsilon''=\frac{\delta_0}{\varepsilon_0\omega^{1-s}}, \tag{1}$$

where δ_0 and s are the fitting parameters and ε_0 is the dielectric permittivity in free space. The solid lines in Figs. 5 and 6 represent theoretical fitting curves with Eq. (1). The frequency exponent (s) is found to be 0.131 and 0.128, respectively, for the SmA and SmC^* phases. These values of s indicate hopping conduction behavior of the carriers [16] in the sample. The estimated values of δ_0 are 2.06×10^{-10} and 8.32×10^{-10} Ω cm^{-1} respectively, for the SmA and SmC^* phases.

So far, we have discussed quantitatively the temperature and frequency dependences of two components of dielectric permittivity ε' and ε'' showing dielectric anomaly in the ferroelectric phase of the CS-1013 mixture. We are presenting below the dielectric relaxation processes in terms of the

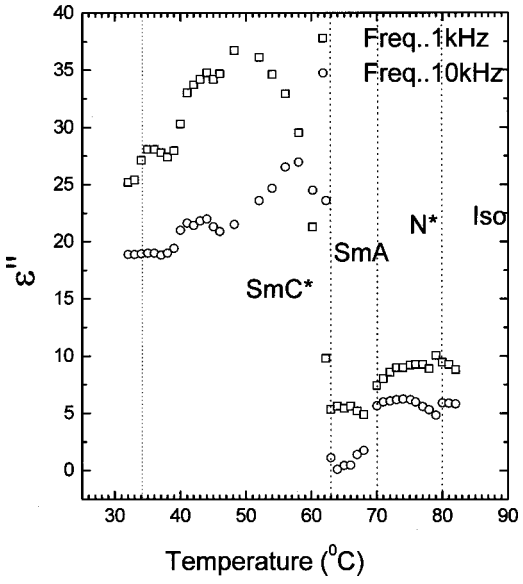

FIG. 1. Temperature-dependent dielectric loss (ε'') of ferroelectric CS-1013 for two fixed frequencies showing different mesophases.

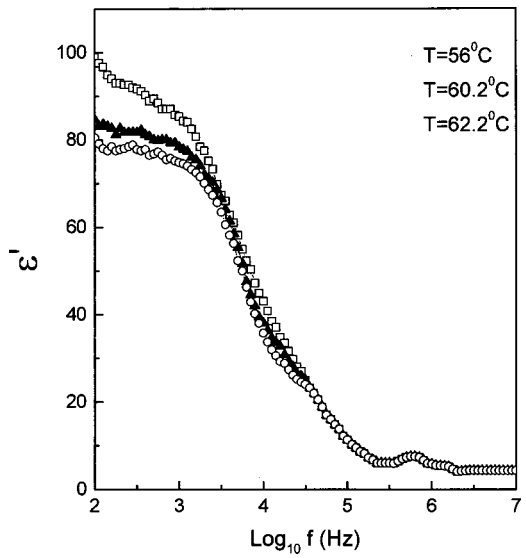

FIG. 2. Frequency dependence of the real part of dielectric constant (ε') in the ferroelectric SmC^* phase at different fixed temperatures at zero bias.

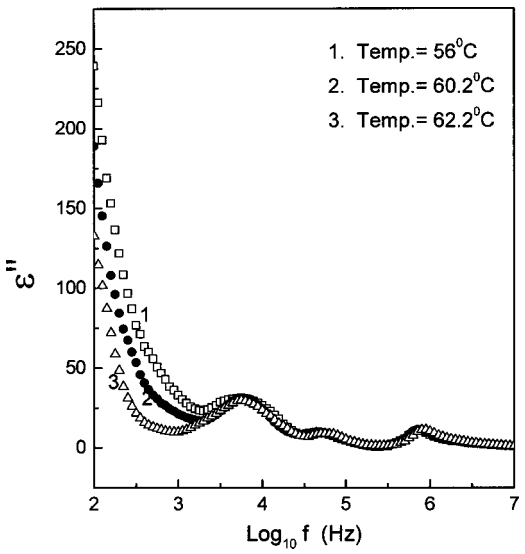

FIG. 4. Frequency dependence of the imaginary part of dielectric constant (ε'') in the ferroelectric SmC^* phase at different fixed temperatures.

Goldstone mode [17,18] and soft mode [19]. The dielectric spectra of the SmC^* phase of the CS-1013 mixture measured in the frequency range 100 Hz–10 MHz clearly indicated (Fig. 1) the para to ferroelectric SmA-SmC^* phase transition occurring at $T_C = 63\,^{\circ}\mathrm{C}$. The dielectric spectrum connected with the Goldstone mode has been shown in the form of the dispersion and absorption curves in Figs. 2 & 4 as discussed above. The corresponding Cole-Cole diagrams near the SmA-SmC^* phase-transition region is shown in Fig. 7. We first fit the experimental points (○ and ▲) with Cole-Cole modification [20] of the Debye equation written as

$$\varepsilon^* = \varepsilon_\infty + \frac{\varepsilon_s - \varepsilon_\infty}{1 + (i\omega\tau)^{1-\alpha}}, \tag{2}$$

where ε_s is the static dielectric constant, ε_∞ is the high-frequency dielectric permittivity, $\tau (= 1/2\pi f_c)$ and α are, respectively, the dielectric relaxation time and the distribution parameter, f_c is the relaxation peak frequency. Solid lines in Fig. 7 are the theoretical fitting curves with Eq. 2. Table II contains the corresponding fitting parameters for the Goldstone mode in the SmC^* phase.

It may be seen from Figs. 2 and 4 (obtained for the SmC^* phase) that there is a pronounced dispersion near 5 kHz connected with the Goldstone mode. However, near the (SmA

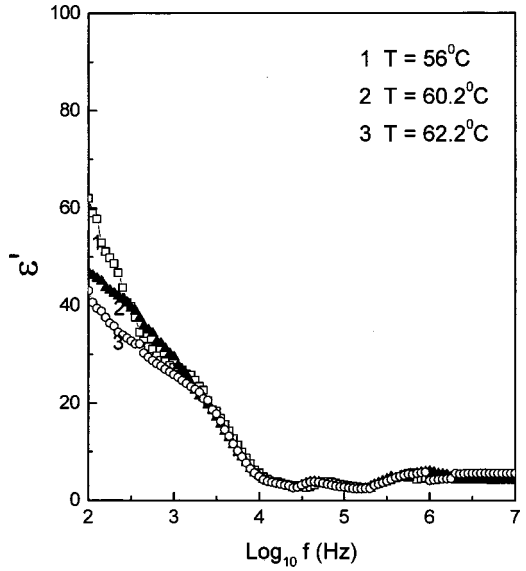

FIG. 3. Frequency dependence of the real part of dielectric constant (ε') in the ferroelectric SmC^* phase at different fixed temperatures with bias (=1.0 V).

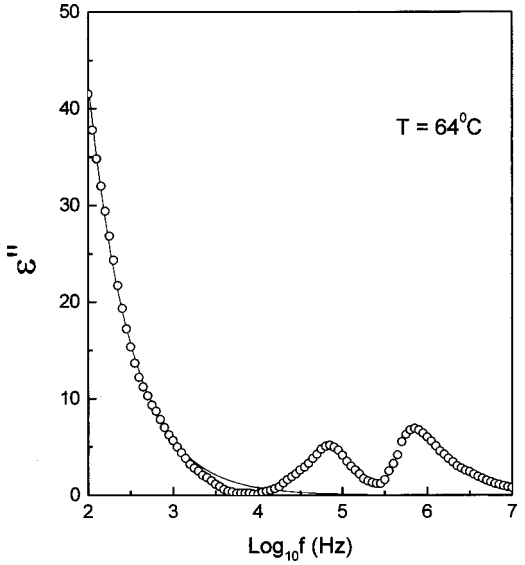

FIG. 5. Frequency dependence of the imaginary part of dielectric constant (ε'') in paraelectric SmA phase at 64.0 °C. The solid line shows the conductivity contribution [according to Eq. (1)].

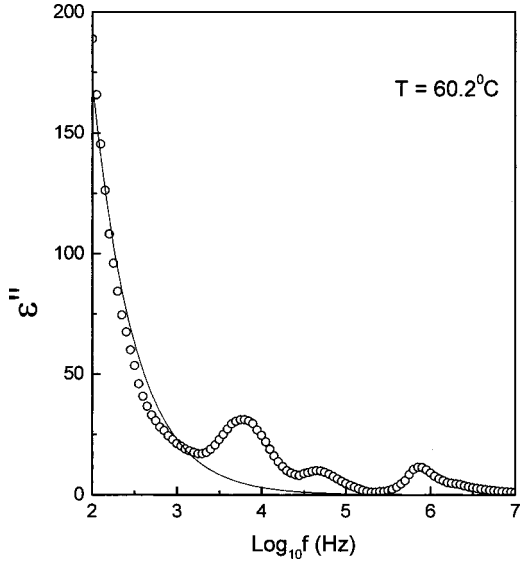

FIG. 6. Frequency dependence of the imaginary part of dielectric constant (ε'') in the ferroelectric SmC^* phase at 60.2 °C. The solid line shows the conductivity contribution [according to Eq. (1)].

$\rightarrow$SmC^*) transition region, another mode is present, which is knows as the soft mode. But for the present sample its dispersion takes place at much higher frequencies near 50 kHz. In the SmA phase (Fig. 5), the Goldstone mode disappears and the soft mode contribution appears. One may conclude from the temperature-dependent dielectric constant data (Fig. 1) that a ferroelectric first-order phase-transition course at 63 °C. In Fig. 8, the soft mode is presented in the form of Cole-Cole modification of the Debye equation (2) for the SmC^* and SmA phase, respectively. The scattered points in Fig. 8 represent the experimental points and the continuous line represents the theoretical fit with Eq. (2). The fitting parameters have been shown in Table III.

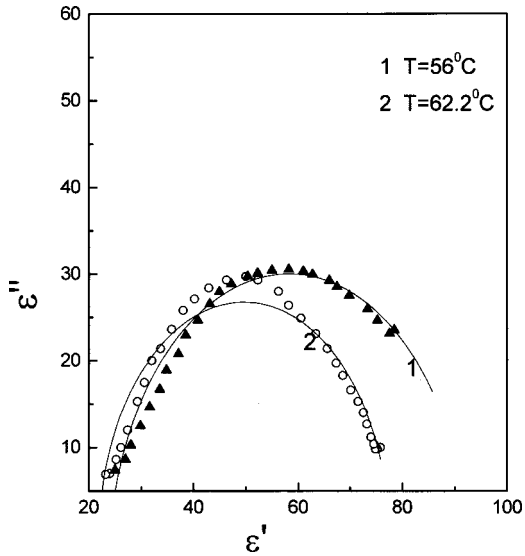

FIG. 7. Cole-Cole diagrams obtained for the Goldstone mode in the SmC^* phase.

TABLE II. Dielectric relaxation parameters corresponding to the Goldstone mode.

T (°C)	ν (Hz)	τ (μs)	ε_s	ε_α	α
56	5623.41	28.3022	88.768	28.08	0.0127
58	5011.87	31.7555	87.93	24.51	0.0314
60.2	5623.41	28.3022	79.137	26.957	0.009
62.2	5623.41	28.3022	77.17	21.064	0.0286

It is well known that in polar liquid crystals, two principal molecular reorientations, viz., the reorientations around the short and long molecular axes, generate separate dielectric relaxation regions falling within radio and microwave frequency ranges [21,22]. From our experimental data, it is clearly seen that both molecular motions give contributions to the dielectric permittivities. In this case, the molecular relaxation in both SmA and SmC^* phases have the same frequency range near MHz region.

The Goldstone mode and the soft mode critical frequencies as a function of temperature are plotted in Fig. 9(a). By plotting the soft mode critical frequency (ν_c^s) as a function of temperature, straight lines are obtained in the both paraelectric (SmA) and ferroelectric (SmC^*) regions [Fig. 9(b)]. This result may be explained by molecular-field approximation [23]. According to this approximation, the critical frequency of the soft mode should follow the following relation:

$$\nu_c^s = a(T\text{-}T_C) + b, \tag{3}$$

where a and b are constants. According to this approximation, the slope ratio is predicted to be two. In the case of the CS-1013 mixture, the slope ratio is about 1.106 and the intercept is of about 60 kHz. So, the frequency of the soft mode extrapolated to the transition temperature at zero-momentum transfer ($q=0$) has a finite value and this corroborates the theory. However, the ratio of the slopes is 44.7% lower than the theoretical value. The two soft mode

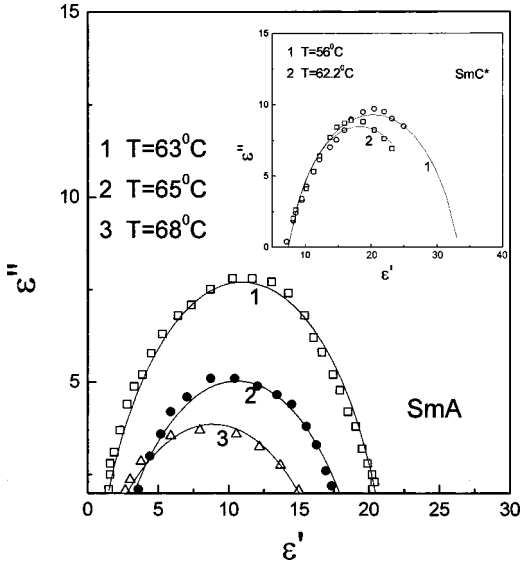

FIG. 8. Cole-Cole diagrams obtained for soft mode in the SmC^* and SmA phases.

TABLE III. Dielectric relaxation parameters corresponding to the soft mode.

Phase	T (°C)	ν (Hz)	τ (μs)	ε_s	ε_α	α
SmC*	56	44 668.35	3.56	33.29	7.37	0.2067
	58	44 668.35	3.56	44.5	6.16	0.41
	60.2	44 668.35	3.56	32.41	8.06	0.317
	62.2	56 243.35	2.83	28.07	7.71	0.106
SmA	63	63 095.72	2.52	21.28	0.637	0.184
	64	70 794.56	2.25	20.211	0.839	0.41
	65	79 432.8	2.0	19.45	1.71	0.3433
	66	89 125.07	1.786	18.18	1.66	0.359
	68	99 999.97	1.59	17.27	0.53	0.4496

branches of the relaxation frequency in SmC* and SmA phases in the present FLC meet at the Curie temperature $T_C = 63.9\,°\mathrm{C}$ which is about 0.9 °C higher than the T_C ($=63\,°\mathrm{C}$) observed from texture study under polarizing microscope [24]. This indicates that the T_C obtained from the extrapolation of the two relaxation frequency branches of the soft mode in SmC* and SmA phases are almost equal within experimental error. The very small difference of T_C ($\Delta T_C = 0.9\,°\mathrm{C}$) between texture and dielectric studies might be associated with the less importance of the biquadratic coupling term in the present ferroelectric CS-1013 mixture.

Thus, in the present SmA-SmC* phase of the CS-1013 mixture, the observed high contribution to the dielectric permittivity was assigned to the Goldstone mode showing an Arrhenius-type behavior of the critical frequency. In the vicinity of the SmA-SmC* transition point, the Goldstone mode contribution to the dielectric constant is almost constant. The little deviation (around 0.9 °C) between T_C determined experimentally and T_C observed from texture indicates small biquadratic coupling for this ferroelectric smectic mixture. We suggested below a theoretical model for the analysis of the ferroelectric phase transition in a liquid crystal.

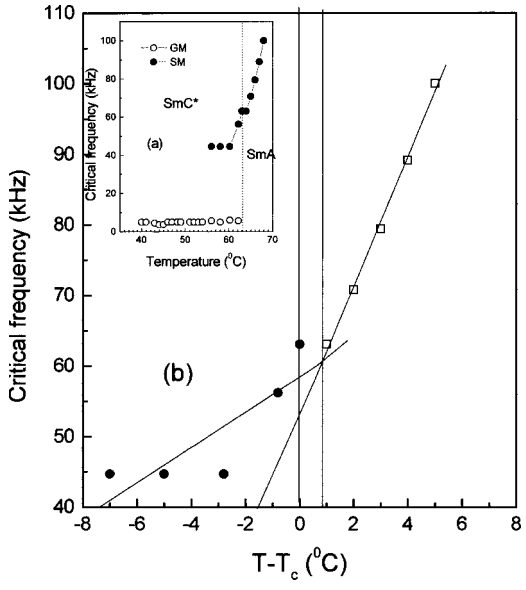

FIG. 9. (a) Variation of critical frequency of Goldstone mode and soft mode with temperature in SmC* and SmA phases. (b) Temperature dependence of the soft mode critical frequency in the vicinity of the SmA-SmC* transition of the ferroelectric smectic mixture (CS-1013).

B. Suggestion for a pseudospin model for the study of ferroelectric and other properties in ferro and antiferroelectric liquid crystals

The recent discovery of ferroelectric (FE) and antiferroelectric (AFE) or ferrielectric (FI) behavior in liquid crystalline materials is very interesting as well as important. Ferroelectric and antiferroelectric phase transitions in crystalline solids as in many hydrogen bonded (H-bonded) systems are very well known [25]. The FE and AFE properties in crystalline materials have been well represented using the concept of spin (better called ''pseudospin'') in analogy with magnetic spin. The pseudospin concept in FE was first introduced in crystalline medium by De Gennes [26] and Blinc and Zeks [27] and subsequently such a pseudospin concept has been widely applied to many FE and AFE crystals [27] with success. During the last decade, different theories of FE and AFE structures in different compounds and mixtures have been proposed [28–33]. In many binary mixtures, for example, MHPOOCBC and EHPOCBC, different possible phases are observed [32,34]. These phases are designed as SmC_A^*-SmC_γ^*-FI$_\mathrm{H}$-AF-SmC_α^*-SmA. The phase Sm$C\alpha$* is considered as a coexistence of a variety of FE and AFE structure [35–37]. However, the origin of such fluctuating phases is not very clear. The appearance of the FI$_L$-Sm$_\gamma$-FI$_\mathrm{H\text{-}AF}$ was described by one-dimensional (1D) Ising model with long repulsive interaction [34]. But 1D Ising model is not at all sufficient to describe the quasi-2D or 3D character of the FLC. Isozaki and coworkers [34] suggested that this sequence of phase transitions revealed the devil's staircase [38,39] intrinsic to these materials. Furthermore, they also tried to interpret the successive SmC* to SmC_A^* phase transitions by the devil's staircase occurring in the Ising model with long-range repulsive interaction [38,39]. Here, the Ising spins are considered to represent not a real molecular state, but the pair state of two neighboring layers. This is actually the ''pseudospin'' concept, mentioned above, used by several authors [26,27] to explain FE

or AFE phase transitions even in nonmagnetic hydrogen-bonded crystals. The repulsive interactions between two separate pairs of systems used by Matsumoto *et al.* [40] are quite arbitrary. However, recently, Yamashita and Miazima [41] used another type of devils's staircase model, the axial next-nearest-neighbor Ising model (ANNNI), viz.,

$$\mathrm{H}=-J_1\Sigma_{ij}\sigma_i\sigma_j-J_2\Sigma^A_{ij}\sigma_i\sigma_j-J_3\Sigma^A_{ij}\sigma_i\sigma_j, \tag{4}$$

where the spin component σ_I takes values ± 1 and J values are exchange parameters, the sign and magnitude of which designate the ferro, ferri, or antiferroelectric phase transitions. In this model, the AFE second-neighbor interaction is considered negative ($J<0$). Yamashita and Miazima [41] also pointed out that in the absence of an external field, by adjusting the coordinate system to the helix of chiral smetics and changing it along the helical axis, the state of the layer in different phases may be expressed only by two points on the projection space P^2, corresponding to the directions of inclination of *n*, the director field (considered uniform in a smectic layer). They, however, did not give importance to the change of the angle between *n* and the layer normal at the phase transitions among Sm*A*, Sm$C\alpha$*, and Sm*C**. This model [Eq. (1)] actually used the fluctuation of the exchange interaction only to show different phase transitions in liquid crystalline system of interest.

However, we believe that there is close resemblance between the FE or AFE phase transition occurring in many H-bonded crystals and in the FE or AFE liquid crystals, and the phase transitions in the liquid crystalline state could be due to the successive fluctuations of tilt angle and magnitude of the pitch with change of temperature or other stimulating agents (such as electric field, pressure, etc.). So if some variables related only to the tilt angle and the pitch are introduced in the expression of the Hamiltonian describing the FE or AFE phase transition in crystalline medium, one may investigate the features of FLC, in general. In this case, a spin Hamiltonian may be used to describe FE or AFE phase transitions in liquid crystals. Here, we should note that both tilt angle and the pitch are temperature-dependent fluctuating parameters. Such fluctuations in these parameters will definitely cause (or will be responsible) for the change of polarization and also the exchange interaction between the dipoles, and hence, different types of intermediate phase changes would be possible [as in the Yamashita and Miyazima theory with Eq. (4)] depending on the stability conditions. For this purpose, in the present paper, we are interested to find a form of the pseudospin-type model taking into consideration of the tilt angle (θ) and pitch or wave number, respectively, as biaxiality (b) and uniaxiality (u) parameters (representing biaxiality and uniaxiality of the liquid-crystal molecule) in the Hamiltonian. Here, it is worthwhile to mention that both u and b are temperature- and/or pressure-dependent fluctuating parameters and the pitch and our intention in this section is to show that the said fluctuations will give rise to different phases in the liquid crystalline materials of our interest. The coexistence of a variety of FE and AFE phase in Sm*C** is the cause of these fluctuations. The fluctuation effect in the dynamics of liquid crystals was treated by Kats [42].

In the present paper, our plan is to investigate the ferroelectric phase transitions in FLC with a transverse Ising type of exchange Hamiltonian containing uniaxial and biaxial parameters as mentioned above. Using the Landau theory, we have also attempted to explain, in brief, the nature of FE (for $J>0$) and AFE (for $J<0$) phase transitions. The calculations for polarization, transition temperature, etc., are made using statistical Green's function technique in the domain of the mean-field approximation only.

Let us now consider a model Hamiltonian (anisotropic Heisenberg model or a transverse Ising model with higher-order terms) containing a pseudospin variable along the director as σ_I (with components σ_i^x, σ_i^y, and, σ_i^z, say) and uniaxial parameters (u, which varies with the pitch) and biaxial parameter (b, which varies with the angle θ) having a simplified form

$$\mathrm{H}=-\mu E_i\sigma_i^z\Sigma_i\Sigma_i\sigma_i^z-u\Sigma_i(\sigma_i^z)^2-b\Sigma_{ij}(\sigma_i^x)^2-\Sigma J_{ij}(\sigma_i\sigma_j), \tag{5}$$

where μ is the electric-field (E) -dependent dipole moment along σ_i^z, u is the magnitude of the uniaxiality parameter representing single-molecular anisotropy in the *z* direction of polarization (a measure of the magnitude of pitch), b is the magnitude of the biaxiality parameter representing single-molecular anisotropy transverse to the *z* direction (a measure of the angle θ) and ($J_{ij}>0$ for ferroelectric transition and <0 for antiferroelectric interaction) is the effective exchange interaction between the pseudospins (dipoles) or it is a measure of the interaction strength between u and b (or pitch and θ) at sites i and j. All the three parameters u, b, and J are fluctuating parameters and they are not totally independent of each other with change to temperature, pressure, and other external stimulations. For the purpose of our calculation, we may consider these parameters as independently variable parameters. In order to make the Hamiltonian convenient for theoretical calculation, mean-field type approximation (MFA) is performed so that Eq. (5) may be expressed as a sum of single-molecule Hamiltonian, viz.,

$$\mathrm{H}=\Sigma_i\mathrm{H}_0(i), \tag{6}$$

where

$$\mathrm{H}_0=-\mu\sigma_i^z-u(\sigma_i^z)^2-b(\sigma_i^x)^2-2\Sigma J_{ij}P_s\sigma_i^z, \tag{7}$$

which has the form of transverse Ising model in presence of electric field. To find the statistical averages of σ_i^z, σ_i^x, etc., we used the statistical Green's function technique of Zubarev [43] similar to our earlier work [44] and the spectral theorem. The higher-order Green's function are decoupled by the RPA (random-phase-approximation) type decoupling scheme [45]. Using this Hamiltonian [Eq. (7)], the average spontaneous polarization P_s related to the statistical average $\langle\sigma_i^z\rangle$ is expressed as

$$P_s=\langle\sigma_i^z\rangle=\mathrm{Tr}\exp[-\beta\mathrm{H},\sigma_i^z]/\mathrm{Tr}\exp(-\beta\mathrm{H}). \tag{8}$$

$\langle\ \rangle$ indicates statistical average of of the enclosed operator, $\beta=1/(k_BT)$, k_B is the Boltzmann constant and T is the absolute temperature. The corresponding energy spectrum with the Hamiltonian is given by

$$E_0=-2b \quad \text{and} \quad E_{1,2}=-u-b\pm\lambda,$$

$$\lambda=[\mu+2P_s^2\eta J+b^2]^{1/2}. \tag{8a}$$

We have used, for simplicity, $J=\Sigma J_{ij}$ as the interaction strength between the ith site and each with its η nearest neighbor. We also use $\langle\sigma_i^z\rangle=\langle\sigma_j^z\rangle=\sigma$. Now, following the standard procedure [45] the expression for the average polarization [from Eq. (8)] comes out to be of the form

$$P_s\sim[1-(b/\lambda)^2][\tanh\beta\lambda/(1+\exp\{-\beta(u-b)\}/2\cosh\beta\lambda)]. \tag{9a}$$

At $T=T_C$ (ferroelectric Curie temperature), Eq. (9a) gives the ferroelectric transition temperature, viz.,

$$\tanh\beta_C\lambda_C/(1+\exp\{-\beta_C(u_C-b_C)\}/2\cosh(\beta_C\lambda_C)=0, \tag{9b}$$

where the suffix C indicates values at the transition temperature. The expression of spontaneous polarization [Eq. (9a)] can be fitted with the experimental data of FLC. This expression is similarly valid for the solid materials where there is no fluctuation of the parameters (one obtains only single sets of fitting parameters). Thus, we see from Eq. (9) that P_S is dependent on u and b, i.e., pitch and the tilt angle, respectively. J is introduced through λ. So, from fitting of the experimental data of polarization, transition temperature, etc. with Eqs. (9a), (9b), it would be possible to get the static values of the tilt angle and the pitch or wave numbers at various temperature, pressure, etc. However, we did not attempt for such calculations in this paper, as our intention is to show applicability of such a pseudospin model for explaining ferroelectric and also successive phase transitions. The dielectric susceptibility χ may also be calculated for the statistical Green's function using Kubo's theory [46], which will be shown elsewhere. The average value of the square of single-site polarization is a measure of short-range order in FLC may be written as

$$r_p=\langle(\sigma_i^z)^2\rangle=\tanh\beta\lambda/[1+\exp\{-(\beta(u-b)/2(\cosh\beta)\}], \tag{10}$$

where $\langle\sigma_i^z)^2\rangle$ is the short-range order parameter depending on uniaxial and biaxial parameters.

To study the nature of the phase transition, the free energy of the system (F) may be obtained from the MFA using the following equation:

$$-\beta F=\ln\exp(-\beta). \tag{11}$$

Therefore, one has from free energy

$$\partial(-\beta F)/\partial(\beta\mu)=NP_s,\partial(-\beta F)/\partial(\beta u)=Nr_p,\partial(-\beta F)/\partial(\beta K\eta)=NP_s^2,$$

where N is the number of dipolar molecules or ions in the system. Using Eqs. (8) and (11), we may write the free energy (at zero external field) as

$$f=F/NK=P_s^2-(1/\beta J)\ln[\exp(2BU)+2\exp(\beta J\phi)\cosh(2\beta J)(P_s^2+B^2 2)^{1/2}], \tag{12}$$

where the parameters $J=\beta N k_B$. $B=b/N k_B J$, $\phi=J+U$ and $U=u/NJ$.

The ferroelectric transition temperature T_c ($\langle\sigma^z\rangle\to 0$ at $T\to T_c$) is obtained from

$$2[\sinh(\beta_cJB)-\cosh(\beta_cJB)]=\exp[-\beta_cJ(D-B)], \tag{13}$$

where $\beta_c=1/k_BT_c$.

Within the mean-field approximation, the Landau theory [47] of phase transition is generally used. The free-energy difference between the finite and zero polarization state is given by

$$\Delta f=f(P_s)-f(P_s=0) \tag{14}$$

$$=P_s^2-(1/\beta J)\ln[\{\exp(-\beta J\phi)+2\cosh(2\beta J)(P_s^2+B^2/4)^{1/2}\}/\{\exp(-\beta J\phi)+2\cosh(\beta JB)\}]. \tag{15}$$

One can compare Eq. (15) with the following Landau equation:

$$\Delta f=\alpha P_s^2+\gamma P_s^4\delta P_s^6+(\text{higher-order terms})\times(\text{neglected for simplicity}), \tag{16}$$

where α, γ, and δ are usual parameters that may be obtained by expanding Eq. (15) in powers of polarization and then comparing with Eq. (16). These parameters are functions of J, u, and b. For a second-order transition, one has $\alpha=0$, which gives

$$\exp(\beta J\phi)+2\cosh(\beta JB)-(4/B)\sinh(\beta JB)=0. \tag{16a}$$

Again, the additional condition for the second-order transition is $\gamma\geqslant 0$ or

$$\exp(\beta JL)\leqslant[\sinh(2BL)]/\beta B\cosh(2\beta Bb)\sinh(\beta B), \tag{17}$$

where $(L=U-B)$ must hold. When the second-order transition becomes first order, the above inequality becomes an

equality. This is the critical point denoted by the suffix c. For this critical point to appear one has $\delta_c > 0$ or

$$32[\psi_c + \cosh(\beta_c J_c B_c)]^2[(\beta_c J_c (B_c^3)(1/B_c^2) + [(\beta_c^2 J^2/3B_c^2)\sinh(\beta_c B_c) - (\beta_c^2 J^2/B_c^4)\cosh(\beta_c J_c B_c)] - 32(\beta_c J_c/B_c)^2 \sinh(\beta_c J_c B_c)][\psi_c + \cosh(\beta_c B_c)] \times \{\beta_c J_c (B_c)\cosh(\beta_c J_c B_c) - (1/B_c)^2 \sinh(\beta_c J_c B_c)\} + \{4\beta_c J_c (27B_c)\sinh(\beta_c J_c B_c)\} > 0, \quad (18)$$

where $\psi_c = -(U_c - B_c)/2$, $\beta_c = 1/k_B T_c$ (T_c is the critical temperature). Now, from the minimization of the free energy, one has to find the thermodynamic stability using the following condition:

$$\partial f/\partial P_s = 0, \quad (19a)$$

and

$$\partial^2 f/\partial P_s^2 \geqslant 0. \quad (19b)$$

The first derivative (19a) gives polarization similarly to [Eq. (9)] and so need not be written again. The second condition (19b) gives the stability conditions, viz.,

$$2[1 + 2\beta J(P_s^2 + B^2/4)]\tanh(2\beta J)(P_s^2 + B^2/4)^{1/2} - 4\beta J(P_s^2 + B^2/4)^{1/2} \geqslant 0. \quad (20)$$

For the thermodynamic solution of P_s, the above inequality [Eq. (20)] must be satisfied. When the equality holds, the solution to Eq. (20) gives a line of critical points for a given value of B, which is a function of the tilt angle (θ), in particular. To investigate the first-order transition as the temperature approaches zero, the free-energy difference (Δf) is expanded in the limit that $P_s \to 1$ (maximum) and $\beta J \to \infty$ (maximum). This expansion gives a maximum value for the U parameter, viz.,

$$|U|_{\max} = B - 1 + 2(1 + B^2/4)^{1/2}, \text{ with } 2(1 + B^2)^{1/2} > |U| > B. \quad (21)$$

The solution for [Eq. (20)] gives a family of stability curves as B increases from zero. It is found that the thermodynamic solutions for P_s exist above such stability curves. For a critical value of B, there is a critical value of βJ (the normalized critical temperature) for $P_s \to 0$. The values of U are the critical points for the first order transition in a FLC. Here, we should note that the biaxial parameter, i.e., contribution from the tilt angle variation, must not be an appreciable function of the uniaxial anisotropy parameter, i.e., pitch or wave number. Otherwise, dipolar ordering could cease to exist (in case of zero external field). For this reason, the contributions from the two types of anisotropy parameters would be opposite in sign. For the minimum values of U, the straight line nature of the curve is indicated from the solution of Eq. (21). In case of no biaxial anisotropy (i.e., tilt angle independent or constant) first-order transition takes place in the range $-1.5 \leqslant U_c \leqslant -1$ and $0 \leqslant (\beta_c J)^{-1} \leqslant 0.75$ (approximately).

It is further noted that for different values of U and B, both first- and second-order phase transitions are observable. For the critical value of B larger than that of the first-order transition, polarization curves continues from zero to one. However, as the critical value of B increases, the possibility of first-order transition increases. For the critical values of B greater than those of the critical values of the first transition, polarization jumps from zero to higher values. Here, there exists the possibility of tricritical behavior under pressure or other external field. The situation resembles that of solid-state ferroelectric material KH_2PO_4[27] where similar tricritical behavior has been observed under pressure. Thus, from the present theoretical model with uniaxial and biaxial anisotropies, one could expect tricritical behavior even in FLC, which was already reported [27].

Finally, we should note that the fluctuations of B and U parameters, which are functions of the tilt angle and the pitch of the FLC, affect the polarization, and hence, in the appearance of the sequence of phase transitions observed in the present CS-1013 and similar other systems. Interestingly, the combined effect of fluctuations of both B and U may also be used to show the re-entrant polarization behavior in FLC (not shown in this paper). Further, to note that using the Kubo theory [46] and standard relations, one may calculate dielectric constant, piezoelectric coefficient, etc., which would be discussed elsewhere.

In conclusion, it is suggested that within the constraints of the MFA, the Heisenberg Hamiltonian (or a transverse Ising-type model) with uniaxial and biaxial anisotropic terms may be used to study ferroelectric (or antiferroelectric) behavior in liquid crystals. Fluctuations in both the tilt angle (associated with the biaxial parameter, B) and the pitch (associated with the uniaxial parameter, U) around their mean values (equivalent to the corresponding crystalline values) have a large effect on the polarization, the nature of phase transition, and phase behavior of the system. Moreover, consideration of the fluctuation of these two parameters in the Hamiltonian would cause the polarization to go from continuous to discontinuous values. Simultaneous fluctuations of both B and U might also exhibit many features in liquid crystals.

ACKNOWLEDGMENTS

One of the authors (B.K.C.) is grateful to the AvH Foundation Germany, for providing the HP4192A frequency analyzer and the Eurotherm temperature controller used for this work. One of the authors (S.K.K.) is also grateful to CSIR, Government of India, for financial assistance. The authors (B.K.C. and S.K.K.) gratefully acknowledge Mr. Somnath Roy for his help in the computer software development.

[1] R. B. Meyer, L. Liebert, L. Strzelecki, and P. Keller, J. Phys. (France) Lett. **36**, L69 (1975).
[2] A. D. L. Chandani, T. Hagiwara, Y. Suzuki, Y. Ouchi, H. Takezoe, and A. Fukuda, Jpn. J. Appl. Phys., Part 2 **27**, L729 (1988).
[3] J. Pavel, M. Glogarová, and S. S. Bawa, Ferroelectrics **76**, 221 (1987).
[4] A. Ezcurra, M. A. Pérez Jubindo, M. R. Fuente, J. Etxebarria, A. Rémon, and M. J. Tello, Liq. Cryst. **4**, 125 (1989).
[5] C. Legrand and J. P. Parneix, J. Phys. (Paris) **51**, 787 (1990).
[6] T. Carlsson, B. Zeks, C. Filipic, and A. Levstik, Phys. Rev. A **42**, 877 (1990).
[7] J. Hoffmann, W. Koczynsk, and J. Malecki, Mol. Cryst. Liq. Cryst. **44**, 287 (1978).
[8] M. Glogarova, J. Pavel, and J. Fousek, Ferroelectrics **55**, 117 (1984).
[9] B. Zeks, A. Levstik, and R. Blinc, J. Phys. (Paris), Colloq. **40**, C3-409 (1979).
[10] A. Levstik, T. Carlsson, C. Filipic, I. Levstik, and B. Zeks, Phys. Rev. A **35**, 3527 (1987).
[11] A. M. Biradar, S. S. Bown, C. P. Sharma, and Subhas Chandra, Jpn. J. Appl. Phys., Part 1 **30**, 2535 (1991).
[12] K. Kondo, T. Kitamura, M. Isogai, and M. Mukoh, Ferroelectrics **85**, 361 (1988).
[13] B. Zeks, Ferroelectrics **53**, 33 (1984).
[14] M. A. Pérez Jubindo, A. Ezucer, J. Etxebarria, A. Remón, M. J. Tello, M. Marcos, and J. L. Serrano, Mol. Cryst. Liq. Cryst. **159**, 137 (1988).
[15] S. U. Vallerien, F. Kremer, B. Hueser, and H. W. Spiess, Colloid Poly. Sci. **267**, 583 (1989).
[16] N. F. Mott, and E. A. David, *Electron processes in Non Crystalline Materials*, 2nd ed. (Clarendon, Oxford, 1979).
[17] A. M. Biradar, S. Wróbel, and W. Haase, Phys. Rev. A **39**, 2693 (1989).
[18] M. Pfeiffer, G. Soto, S. Wróbel, W. Haase, R. Twieg, and K. Vetterton, Ferroelectrics **121**, 55 (1991).
[19] S. Wróbel, A. M. Biradar, and W. Haase, Ferroelectrics **100**, 271 (1989).
[20] K. S. Cole and R. H. Cole, J. Chem. Phys. **9**, 341 (1941).
[21] H. Kresse, *Advances in Liquid Crystals*, edited by Glenn H. Brown (Academic, New York, 1983), Vol. 6.
[22] J. P. Parneix, C. Legrand, and D. Decoster, Mol. Cryst. Liq. Cryst. **98**, 361 (1983); S. Wróbel, *ibid.* **127**, 67 (1985).
[23] R. Blinc and B. Zeks, Phys. Rev. A **18**, 740 (1978).
[24] T. Minato and K. Suzuki, Liq. Cryst. **23**, 43 (1997).
[25] E. M. Lines and A. M. Glass, *Principles and Applications of Ferroelectrics and Antiferrielectrics* (Clarendon, Oxford, 1977).
[26] P. G. de Gennes, Solid State Commun. **1**, 132 (1963).
[27] R. Blinc and B. Zeks, Adv. Phys. **21**, 693 (1972).
[28] J. W. Goodby, J. Mater. Chem. **1**, 307 (1992).
[29] A. D. L. Chandani, E. Gorecka, Y. Ouchi, H. Tokezoe, and A. Fukuda, Jpn. J. Appl. Phys., Part 2 **28**, L1265 (1989).
[30] H. M. Fukai, Y. Yamada, N. Yamamoto, and Y. Ishibashi, Jpn. J. Appl. Phys., Part 2 **28**, L849 (1989).
[31] J. W. Goodby, J. S. Patel, and E. Chin, J. Mater. Chem. **2**, 197 (1992).
[32] A. S. Pikin, S. Hiller, and W. Haase, Mol. Cryst. Liq. Cryst. **262**, 425 (1995).
[33] H. Orihara and Y. Ishibashi, Jpn. J. Appl. Phys., Part 2 **29**, L115 (1990).
[34] T. Isozaki, T. Fujiwara, H. Tokezoe, A. Fukuda, H. Hagiwara, Y. Suzuki, and I. Kawamura, Jpn. J. Appl. Phys., Part 2 **31**, L1435 (1992).
[35] Y. Takanishi, K. Hiroaka, V. K. Agrawall, H. Tokezoe, A. Fukuda, and M. Matsushita, Jpn. J. Appl. Phys., Part 1 **130**, 2023 (1991).
[36] K. Hiroueka, Y. Takanishi, K. Skarp, H. Tokezoe, and A. Fukuda, Jpn. J. Appl. Phys., Part 2 **30**, L1819 (1991).
[37] T. Ishuzaki, K. Hiroaka, Y. Takanishi, H. Tokezoe, A. Fukuda, Y. Suzuki, and I. Kawamura, Liq. Cryst. **12**, 59 (1992).
[38] P. Bak and J. Boehm, Phys. Rev. B **21**, 5297 (1980).
[39] P. Bak and R. Bruin, Phys. Rev. Lett. **49**, 249 (1982).
[40] T. Matsumoto, A. Fukuda, M. Johno, Y. Motoyama, T. Yui, S-S Seomun, and M. Yamashita, J. Mater. Chem. **9**, 2051 (1999).
[41] M. Yamashita and S. Miazima, Ferroelectrics **148**, 1 (1993).
[42] E. I. Kats, Zh. Eksp. Teor. Fiz. **75**, 1819 (1978) [Sov. Phys. JETP **48**, 916 (1978)]; *ibid.* **32**, 1004 (1971).
[43] D. N. Zubarev, Usp. Fiz. Nauk. **71**, 71 (1960) [Sov. Phys. Usp. **3**, 320 (1960)].
[44] K. R. Chowdhury, D. K. Nath, and B. K. Chaudhuri, Phys. Rev. B **26**, 6276 (1982).
[45] S. Banerjee, D. K. Nath, and B. K. Chaudhuri, Phys. Rev. B **24**, 6469 (1981); N. N. Bogolynbov and S. V. Tyablikov, Sov. Phys. Dokl. **4**, 604 (1959).
[46] R. Kubo, J. Phys. Soc. Jpn. **12**, 570 (1957); M. Suzuki and R. Kubo, *ibid.* **24**, 51 (1968).
[47] L. D. Landau and E. M. Lifshitz *Statistical Mechanics* (Pergamon, New York, 1978).